A. O. Chingcuanco

Graduate Research Assistant,
Department of Mechanical Engineering,
University of California, Berkeley,
Berkeley, CA 94720

P. M. Lubin

Associate Professor,
Department of Physics,
University of California, Santa Barbara,
Santa Barbara, CA 93106

P. R. Meinhold

Graduate Research Assistant,
Department of Physics.

M. Tomizuka

Professor,
Department of Mechanical Engineering.

University of California, Berkeley,
Berkeley, CA 94720

Modeling and Control of a Balloon Borne Stabilized Platform

A balloon borne stabilized platform has been developed for a remotely operated altitude-azimuth pointing of a millimeter wave telescope system. A modeling and controller design of the azimuth point system of the platform is presented. Simulation results show that the system is capable of continuous operation with pointing rms to better than 0.01 deg. Ground testing results show continuous operation with pointing rms to better than 0.02 deg; while results of the first flight from the National Scientific Balloon Facility (NSBF) at Palestine, Texas show pointing rms better than 0.02 deg.

1 Introduction

A balloon borne stabilized platform is a package that performs altitude azimuth pointing of a telescope system for observations of celestial sources. It is similar in operation to a ground based altitude-azimuth telescope system except that the platform or the gondola is suspended under a 100,000 m³ zero pressure helium filled balloon. The gondola is suspended from a balloon with a flight train of ~ 18 m steel ladder and ~ 36 m parachute, as shown in Fig. 1. The balloon floats at an altitude of about 30 km where it encounters prevailing winds ranging from as low as a couple of knots to 45 knots maximum. Wind directions vary with the time of the year. Ambient temperature is about − 40°C.

There is no active means of controlling the balloon position as it drifts with the wind. A natural rotation of less than a revolution per minute is imparted to the balloon by the atmosphere, and this motion is effectively transferred to the gondola. A natural pendulating motion is experienced by the gondola but this has a slow period and is usually only in the arc minute level at float altitude (Hazen, 1985 and Nigro, 1985). Natural pendulum period is ~ 18 s.

Balloon borne stabilized platforms are used for making astronomical and cosmological observations. It is relatively inexpensive compared to rockets and space shuttle launches. At float altitude of 30 km, noise and fluctuations from the atmosphere are virtually eliminated. Compared to sounding

rockets, balloon flights also offer longer observation time for the experiment.

The stabilized platform described in this paper was developed at the Physics Department of the University of California, Santa Barbara, and is used for sensitive measurements of anisotropy in the Cosmic Background Radiation (CBR), a remnant of the Big Bang.

This paper presents a modeling of the azimuth point system of a stabilized platform. Special features of the hardware are singled out to show how coupling between the balloon and the gondola is minimized. A simplification of the model serves as the basis for designing a PID control with constant desaturation of the flywheel angular velocity. The primary goal of the controller is to achieve azimuth pointing and stabilization of better than 0.1 deg and, the secondary goal is to maintain the flywheel angular velocity below saturation level. Qualitative root locus analyses are used to show the necessity of the desaturation control for continuous operation of the pointing system and also requirement of integral control to remove pointing offset. The implementation of the azimuth pointing system, simulation, ground test, and flight results are discussed.

2 A Model of the Azimuth Pointing System

2.1 Description of Azimuth Pointing Hardware. Figure 2 shows the balloon borne stabilized platform that was designed and built for this project. Azimuth pointing is achieved by torquing directly into inertial space with the use of the reaction wheel system shown in Fig. 3. The flywheel or reaction wheel

Fig. 1 Balloon borne stabilized platform

(not to scale)

100,000 cubic meter zero pressure helium balloon

termination fitting

parachute

steel cable ladder

RCUBE
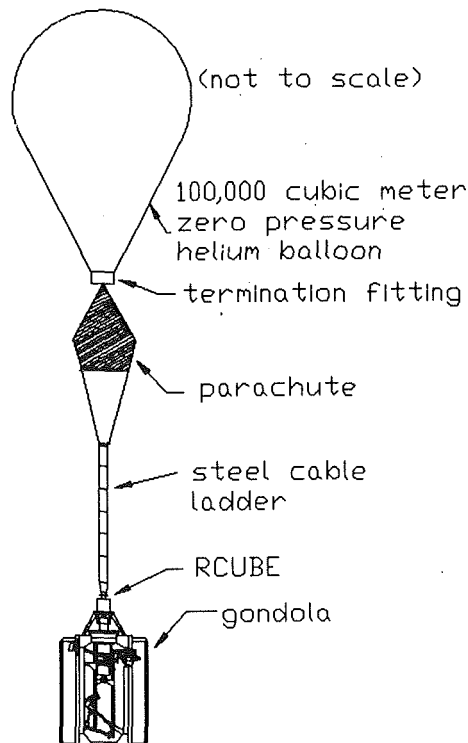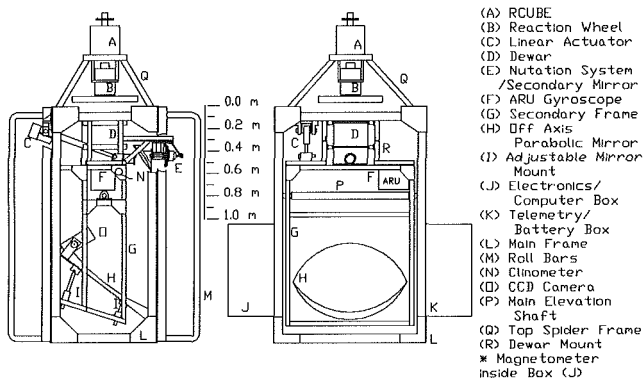
gondola

Fig. 2 Gondola structural layout and main components

(A) RCUBE
(B) Reaction Wheel
(C) Linear Actuator
(D) Dewar
(E) Nutation System /Secondary Mirror
(F) ARU Gyroscope
(G) Secondary Frame
(H) Off Axis Parabolic Mirror
(I) Adjustable Mirror Mount
(J) Electronics/Computer Box
(K) Telemetry/Battery Box
(L) Main Frame
(M) Roll Bars
(N) Clinometer
(O) CCD Camera
(P) Main Elevation Shaft
(Q) Top Spider Frame
(R) Dewar Mount
* Magnetometer inside Box (J)

(A) torque motors
(B) dc tachometer
(C) angular contact bearings (1 pair)
(D) wave spring washer
(E) G-10 plate
(F) top motor housing
(G) bottom motor housing

Fig. 3 Reaction wheel system

(A) torque motor; (B) gear motor;
(C) angular contact bearing (1 pair);
(D) timing belt; (E) three point
flight train connection
* Note: brushes and slip rings not shown

Fig. 4 RCUBE, motor driven double bearing assembly

is spun up by the torque motors causing the gondola to react in the opposite direction. As the reaction wheel operates to keep the gondola pointed correctly, the flywheel will eventually be accelerated to a high angular velocity to the point that the back emf produced prevents any more torquing capability. This condition is referred to as the flywheel reaching saturation. Desaturation can be done by despinning the flywheel, dumping angular momentum to the balloon. Intermittent desaturation, however, can result in the loss of valuable observation time during balloon flight.

To achieve continuous observation time, the reaction wheel is prevented from saturating by employing an active double bearing motor assembly. This device called the RCUBE (Pelling and Duttweiler, 1985), shown in Fig. 4, is an active double bearing assembly that is provided with two motors. The design uses a set of two angular contact bearings, one bearing couples the gondola to the moving race, while the other couples the moving race to the balloon. The d-c gear motor is used to drive the bearing housing in constant motion to avoid stiction during flight. The other motor, a torque motor, is used to torque the gondola against the balloon/flight train system. The RCUBE is used primarily to isolate or to decouple the motion of the gondola from the balloon and to provide a desaturation mechanism for the flywheel angular velocity.
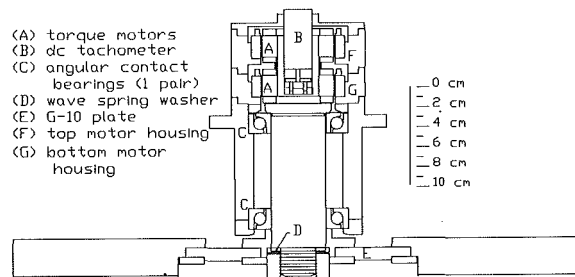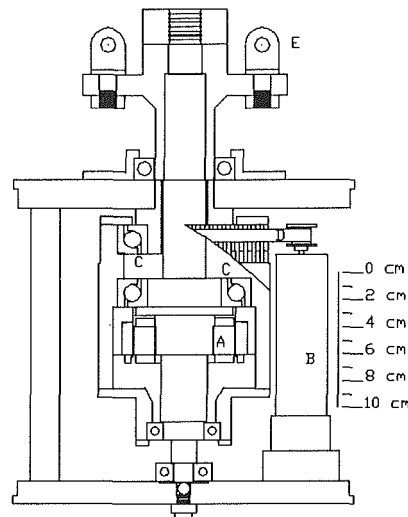
2.2 Dynamic Equations of the Azimuth Pointing System.
Inherent in the modeling process is the assumption that the pendulating motion experienced by the gondola is small enough not to affect the azimuth dynamics of the gondola significantly. This assumption is certainly true at float altitude (Hazen, 1985 and Nigro, 1985), but is not valid during ascent and descent of the gondola.

For modeling, the following assumptions are made.

(1) It is assumed that the dynamics of the motor electrical systems are negligible. This is a reasonable assumption since the azimuth pointing system of the gondola is a slow responding system, considering that the moment of inertia J_g of the gondola is quite large, 195 kg-m^2, compared to the available torque to move it, 5.42 N-m maximum. While the moment of inertia, J_a of the RCUBE's shaft and rotor is small, the RCUBE torque motor and gear motor are expected to be operated with constant or slowly changing command voltages by judicious choice of control.

(2) It is assumed that the timing belt rigidly couples the bearing housing to the gondola frame while at the same time the rotation of the gear motor is transferred without loss to the bearing housing. This assumption is reasonable since the gear motor is expected to be driven with a constant magnitude voltage once the pointing operation begins. While it is true that the bearing housing could experience large fluctuating torques due to oscillations in the command voltage to the RCUBE torque motor, in practice, this command voltage will be computed using a narrow band controller to prevent such rapid response.

(3) Aerodynamic forces including damping on the balloon are negligible. This assumption is reasonable since the balloon
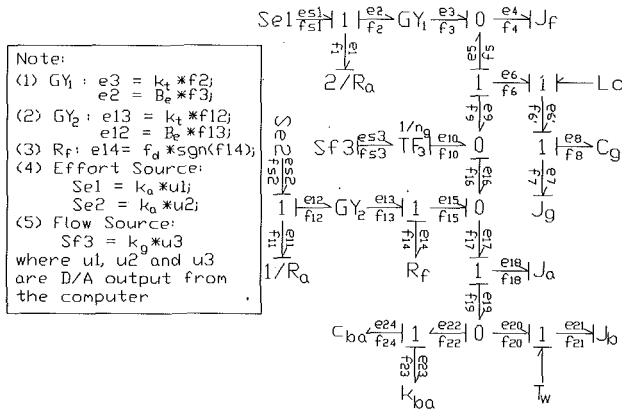
$$Se1\frac{e51}{f51} 1 \frac{e2}{f2} GY_1 \frac{e3}{f3} 0 \frac{e4}{f4} J_f$$

Note:
(1) GY_1 : $e3 = k_t*f2$;
    $e2 = B_e*f3$;
(2) GY_2 : $e13 = k_t*f12$;
    $e12 = B_e*f13$;
(3) R_f: $e14 = f_d*sgn(f14)$;
(4) Effort Source:
    $Se1 = k_a*u1$;
    $Se2 = k_a*u2$;
(5) Flow Source:
    $SF3 = k_g*u3$
where u1, u2 and u3
are D/A output from
the computer

$$SF3 \frac{e53}{f53} 1 \frac{1/n_g}{f3} \frac{e10}{f10} 0 \quad 1 \frac{e8}{f8} C_g$$

$$1 \frac{e12}{f12} GY_2 \frac{e13}{f13} 1 \frac{e15}{f15} 0 \quad J_g$$

$$1/R_a \quad R_f \quad 1 \frac{e18}{f18} J_a$$

$$C_{ba} \frac{e24}{f24} 1 \frac{e22}{f22} 0 \frac{e20}{f20} 1 \frac{e21}{f21} J_b$$

$$k_{ba} \qquad T_w$$

Fig. 5 Bond graph of the azimuth pointing system

and the gondola essentially drift with the wind and the atmospheric pressure at float altitude is near vacuum.

With the three preceding assumptions, a bond graph of the azimuth system is shown in Fig. 5.

Identifying

$f4 = \omega_f$, the angular velocity of the flywheel;
$f7 = \omega_g$, the angular velocity of the gondola;
$f18 = \omega_a$, the angular velocity of the RCUBE shaft/rotor;
$f21 = \omega_b$, the angular velocity of the balloon;
$f16 = \omega_h$, the angular velocity of the bearing housing;

and defining

$T_f = e3 =$ output torque of the reaction wheel system torque motors;
$T_r = e13 =$ output torque of the RCUBE torque motor

the dynamic equations of the azimuth pointing system are derived from the bond graph.

The angular velocity of the bearing housing is written as

$$\omega_h = \omega_g + \omega_m/n_g, \quad \omega_m = k_g*u3 \tag{1}$$

where ω_m is the gear motor azimuth velocity, rad/s; k_g is the combined amplifier and velocity gain, (V/V)(rad/s/V); n_g is the gear ratio between the housing and the drive pinion; and $u3$ is the D/A command output.

With the gear motor turned off, the housing is mechanically grounded to the gondola through the timing belt.

For the RCUBE, the motor output torque, T_r, is

$$T_r = (k_t/R_a)*(k_a*u2 - B_e*(\omega_a - \omega_h)) \tag{2}$$

where k_t is the torque constant, 0.57 N-m/amp; R_a is the armature resistance, 5.7 ohms; k_a is the PWM amplifier gain, 2.6 V/V; B_e is the back emf gain, 0.57 V/rad/s; and $u2$ is the D/A command output.

For the reaction wheel, the motors output torque, T_f, is

$$T_f = (2*k_t/R_a)*(k_a*u1 - B_e*(\omega_f - \omega_g)) \tag{3}$$

where k_t, R_a, k_a, and B_e are as previously described for the RCUBE since the amplifiers and the motors used are the same. The factor 2 is present to reflect the operation of two torque motors working in parallel for the flywheel system; $u1$ is the D/A command output.

Since the flywheel angular velocity is operated at a much higher rate than any velocity rate the gondola is capable of achieving, equation (3) is simplified to

$$T_f = (2*k_t/R_a)*(k_a*u1 - B_e*\omega_f). \tag{4}$$

Coulomb friction torque is mainly due to the relative velocity between the bearing housing and the RCUBE shaft and is written as

$$f_{ga} = -sgn[\omega_a - \omega_h]*f_d \tag{5}$$

or

$$f_{ag} = -sgn[\omega_h - \omega_a]*f_d \tag{6}$$

where f_{ga} is the Coulomb friction torque seen by the RCUBE shaft, f_{ag} is the Coulomb friction torque seen by the gondola/bearing housing, and f_d is the magnitude of Coulomb friction.

The dynamic equation for the balloon is written as

$$J_b d\omega_b/dt = T_w - k_{ba}\int^t (\omega_b - \omega_a)d\tau - c_{ba}*(\omega_b - \omega_a) - c_b*\omega_b \tag{7}$$

where J_b is the balloon moment of inertia, kg-m^2; T_w is the torque disturbance from the atmosphere; k_{ba} is the flight train compliance between the balloon and the RCUBE shaft, N-m/rad; c_{ba} is the flight train damping between the balloon and the RCUBE shaft, N-m/rad/s; and c_b is the damping due to the atmosphere.

For the RCUBE shaft:

$$J_a d\omega_a/dt = T_r - k_{ba}\int^t (\omega_a - \omega_b)d\tau - c_{ba}*(\omega_b - \omega_a) + f_{ga} \tag{8}$$

where J_a is the RCUBE shaft moment of inertia, kg-m^2,
For the gondola:

$$J_g d\omega_g/dt = -T_f - T_r + f_{ag} - c_g*\omega_g + Lo \tag{9}$$

where J_g is the moment of inertia of the gondola, kg$^{(k-g)}$-m^2; c_g is the damping due to the atmosphere, N-m/rad/s; Lo is an external disturbance torque acting on the gondola.

For the flywheel:

$$J_f d\omega_f/dt = T_f \tag{10}$$

where J_f is the flywheel moment of inertia, kg-m^2.

Other than the common but oppositely applied torque, T_r, the gondola and the RCUBE shaft are only related dynamically by the viscous term $(k_t*B_e/R_a)*(\omega_a - \omega_h)$, and the Coulomb friction terms f_{ag} or f_{ga}. The viscous friction is usually small in magnitude. While the Coulomb friction term is not necessarily small, it is limited in magnitude.

Another frictional disturbance is stiction. Stiction is manifested when the relative velocity term, $\omega_a - \omega_h$, is zero. For this model, the stiction is accounted for in the following manner.

For the RCUBE shaft, if $\omega_a - \omega_h$ is zero, the magnitude of the external torque applied to the RCUBE shaft other than the friction term should be greater than the static friction f_s, $|f_s| > |f_d|$. The friction term f_{ga} is then added according to the direction of the impending motion. If the magnitude is not enough to overcome stiction, then the external torque applied to the RCUBE shaft is zeroed out, i.e.,

$$\text{if } \omega_a - \omega_h(> \to \neq)0.0, \text{ then } f_{ga} = -f_d*sgn[\omega_a - \omega_h]$$

$$\text{else if } T_{ext}| < |f_s|, \text{ then } T_{ext} = 0.0 \tag{11}$$

where T_{ext} is the sum of the external torques shown on the right-hand side of equation (8) minus the Coulomb friction term.

The stiction effect on the gondola dynamics is modeled in similar manner.

2.2.1 Constant Rotation Bearing Housing.

The RCUBE is designed as an active suspension system (Pelling and Duttweiler, 1985). One of its primary functions is to keep the Coulomb friction acting in one preferred direction and to prevent the occurrence of stiction due to reversal of bearing rotation. This goal is achieved by driving the bearing housing with the gear motor at a rate faster than any possible balloon rotation rate, and therefore keep the bearings rotating under all conditions of gondola rotation. From equation (5) or equation (6), the direction of Coulomb friction is dependent on $sgn[\omega_a - \omega_h]$. Therefore, if the magnitude of $[\omega_a - \omega_h]$ is always greater than zero, i.e.,

$$\omega_a - (\omega_m/n_g) - \omega_g > 0.0 \tag{12}$$

$$\text{or } \omega_a - (\omega_m/n_g) - \omega_g < 0.0 \tag{13}$$

then the Coulomb friction torque can indeed be made to act

only in a preferred direction. Furthermore, stiction can be avoided provided the magnitude of ω_m/n_g is maintained high enough that any change in $\omega_a - \omega_g$ becomes inconsequential, i.e.,

$$\omega_a - \omega_g > \omega_m/n_g \text{ for } \omega_m < 0 \tag{14}$$

$$\text{or } \omega_a - \omega_g < \omega_m/n_g \text{ for } \omega_m > 0 \tag{15}$$

Both the gondola and the balloon are expected to be slowly rotating systems, but it is possible for the RCUBE torque motor to switch rapidly between positive and negative torques and thus drive the moment of inertia J_a into oscillation. Therefore, it is important that the choice of control scheme to generate $u2$ should prevent or minimize such occurrence especially during steady state operations.

2.2.2 RCUBE Compensation for Friction.
With the frictional disturbance set in one direction, equation (9) could be rewritten as

$$J_g d\omega_g/dt = -(2*k_t/R_a)*(k_a*u1 - B_e*\omega_f)$$
$$- (k_t/R_a)*(k_a*u2 - B_e*(\omega_a - \omega_h)) \pm f_d - c_g*\omega_g + Lo. \tag{16}$$

The frictional disturbance torque can be cancelled by $u2$. In particular, if the viscous friction term $B_e*(\omega_a - \omega_h)$ is neglected as its effect is small, $u2$ can be determined to satisfy

$$-(k_t*k_a*u2)/R_a \pm f_d = 0.0 \tag{17}$$

Thus, if the parameters R_a, k_t, and k_a as well as the Coulomb friction are known completely, $u2$ can be computed to remove or to minimize the effect of the Coulomb friction disturbance.

Defining the angular velocities ω_b, ω_g and ω_a as

$$d\theta_b/dt = \omega_b \tag{18}$$

$$d\theta_g/dt = \omega_g \tag{19}$$

$$d\theta_a/dt = \omega_a \tag{20}$$

equations (7), (8), (9), (10), (18), (19), and (20) are written in matrix form as

$$d[X]/dt = \begin{bmatrix} A11 & A12 \\ A21 & A22 \end{bmatrix}[X] + \begin{bmatrix} B1 \\ B2 \end{bmatrix}[U] + \begin{bmatrix} C1 \\ C2 \end{bmatrix} \tag{21}$$

where

$$[X]^T = [[X1]^T, [X2]^T] = [\theta_b, \omega_b, \theta_a, \omega_a, \theta_g, \omega_g, \omega_f], \tag{22}$$

$$[X1]^T = [\theta_b, \omega_b, \theta_a, \omega_a], \tag{23}$$

$$[X2]^T = [\theta_g, \omega_g, \omega_f], \tag{24}$$

$$[U]^T = [u1, u2], \tag{25}$$

$$[A11] = \begin{bmatrix} 0 & 1 & 0 & 0 \\ \dfrac{-k_{ba}}{J_b} & \dfrac{-c_{ba}-c_b}{J_b} & \dfrac{k_{ba}}{J_b} & \dfrac{c_{ba}}{J_b} \\ 0 & 0 & 0 & 1 \\ \dfrac{k_{ba}}{J_a} & \dfrac{c_{ba}}{J_a} & \dfrac{-k_{ba}}{J_a} & \dfrac{-k_t*B_e}{R_a*J_a} - \dfrac{c_{ba}}{J_a} \end{bmatrix} \tag{26}$$

$$[A12] = \begin{bmatrix} 0 & 0 & 0 \\ 0 & 0 & 0 \\ 0 & 0 & 0 \\ 0 & \dfrac{k_t*B_e}{R_a*J_g} & 0 \end{bmatrix} \tag{27}$$

$$[A21] = \begin{bmatrix} 0 & 0 & 0 & 0 \\ 0 & 0 & 0 & \dfrac{k_t*B_e}{R_a*J_g} \\ 0 & 0 & 0 & 0 \end{bmatrix} \tag{28}$$

$$[A22] = \begin{bmatrix} 0 & 1 & 0 \\ 0 & \dfrac{-c_g-k_t*B_e/R_a}{J_g} & \dfrac{2*k_t*B_e}{R_a*J_g} \\ 0 & 0 & \dfrac{-2*k_t*B_e}{R_a*J_f} \end{bmatrix} \tag{29}$$

$$[B1] = \begin{bmatrix} 0 & 0 \\ 0 & 0 \\ 0 & 0 \\ 0 & \dfrac{k_t*K_a}{R_a*J_a} \end{bmatrix} \tag{30}$$

$$[B2] = \begin{bmatrix} 0 & 0 \\ \dfrac{-2*k_t*k_a}{R_a*J_g} & \dfrac{-k_t*k_a}{R_a*J_g} \\ \dfrac{2*k_t*k_a}{R_a*J_f} & 0 \end{bmatrix} \tag{31}$$

$$[C1] = \begin{bmatrix} 0 \\ \dfrac{T_w}{J_b} \\ 0 \\ \dfrac{k_t*B_e*\omega_m/n_g}{R_a*J_a} - \dfrac{\text{sgn}[\omega_a - \omega_h]*f_d}{J_a} \end{bmatrix} \tag{32}$$

and

$$[C2] = \begin{bmatrix} 0 \\ \dfrac{-k_t*B_e*\omega_m/n_g}{R_a*J_g} - \dfrac{\text{sgn}[\omega_h - \omega_a]*f_d}{J_g} + \dfrac{Lo}{J_g} \\ 0 \end{bmatrix} \tag{33}$$

2.2.3 Flight Line Dynamics.
Neglecting the small effects of $[A12]$ and $[A21]$ in the system matrix $[A]$ in equation (21), eigenvalues of the system matrix can be estimated from $[A11]$ and $[A22]$.

$[A11]$ gives two zero eigenvalues physically corresponding to in phase azimuth motion of the balloon and the RCUBE shaft. The other two eigenvalues can be computed from

$$s^2 + \frac{(\alpha + c_{ba})}{J_a}*s + \frac{k_{ba}}{J_a} = 0 \tag{34}$$

where

$$\alpha = (k_t*B_e)/R_a. \tag{35}$$

The two eigenvalues become

$$\lambda_3, \lambda_4 = \frac{\dfrac{-(\alpha + c_{ba})}{J_a} \pm \left(\left(\dfrac{(\alpha + c_{ba})}{J_a} \right)^2 - \dfrac{4*k_{ba}}{J_a} \right)^{(1/2)}}{2} \tag{36}$$

From equation (36) the vibration mode of the flight train should be asymptotically stable or at least stable.

From $[A22]$, the three remaining system eigenvalues are located at zero, $-(c_g - \alpha)/J_g$ and $(-2*\alpha)/J_f$.

3 Design of PID Control With Constant Desaturation of Flywheel Angular Velocity

The primary design objective is to develop a controller capable of azimuth pointing and stabilization of better than 0.1 deg. A secondary objective is to modulate the flywheel angular velocity to prevent it from approaching saturation level.

Pole placement technique with selective feedback gain is used to design a PID controller with constant desaturation of the flywheel angular velocity.

For design purposes, the following truncated system can be used, i.e.,

$$d[X2]/dt = [A22][X2] + [B2][U] \qquad (37)$$

where

$$[X2]^T = [\theta_g, \omega_g, \omega_f], \qquad (38)$$

$$[U]^T = [u1, u2]. \qquad (39)$$

It is not unreasonable to use the truncated system for controller design for the following reasons.

(1) [A21] has very little cross coupling effect as the only nonzero term is dominated by $1/J_g$.

(2) [A12] has a potentially high coupling term $(\alpha/J_a) * \omega_g$, but the angular velocity of ω_g of the gondola is small especially during steady-state operation. Thus, the effect of [A21] can be neglected.

(3) The effect of the nonlinear friction term, f_{ag}, can be minimized by keeping the velocity of the bearing housing sufficiently large, while friction compensation is provided with the use of the RCUBE torque motor. Residual disturbance can also be eliminated by having an integral control.

The following control law is considered:

$$u1 = -kp * ek - kd * d(ek)/dt - ki \int^t ek * d\tau, \qquad (40)$$

$$u2 = kv * (\omega_f - \omega_{fref}), \qquad (41)$$

$$ek = \theta_{ref} - \theta_g, \qquad (42)$$

where θ_{ref} is the azimuth reference angle; ω_{fref} is the reference flywheel velocity, rad/s; kp, ki, and kd are the proportional (P), integral (I) and derivative (D) gains, respectively, and kv is the desaturation control gain. Time integral of ek is also defined as

$$\theta_i(t) = \int^t \theta ek(\tau) * d\tau, \quad (\theta_i(0) = 0.0). \qquad (43)$$

Augmenting equation (43) into equation (37) and substituting equations (40), (41), and (42) into equation (37), the following equation is obtained:

$$d[X3]/dt = [A33 + B3 * K][X3] - [B3][K][\Theta_{ref}] \qquad (44)$$

where

$$[X3]^T = [\theta_g, \omega_g, \omega_f, \theta_i] \qquad (45)$$

$$[\Theta_{ref}]^T = [\theta_{ref}, \omega_{gref}, \omega_{fref} 0], \qquad (46)$$

$$[A33] = \begin{bmatrix} 0 & 1 & 0 & 0 \\ 0 & \dfrac{-c_g - \dfrac{k_t * B_e}{Ra}}{J_g} & \dfrac{2 * k_t * B_e}{R_a * J_g} & 0 \\ 0 & 0 & \dfrac{-2 * k_t * B_e}{R_a * J_f} & 0 \\ 0 & 0 & 0 & 0 \end{bmatrix} \qquad (47)$$
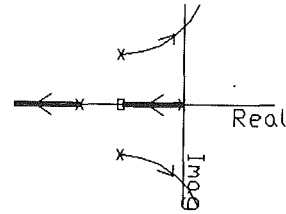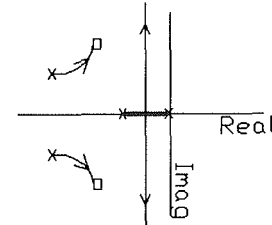
$$[B3] = \begin{bmatrix} 0 & 0 \\ \dfrac{-2 * k_t * k_a}{R_a * J_g} & \dfrac{-k_t * k_a}{R_a * J_g} \\ \dfrac{2 * k_t * k_a}{R_a * J_f} & 0 \\ 0 & 0 \end{bmatrix} \qquad (48)$$

and

$$[K] = \begin{bmatrix} kp & kd & 0 & ki \\ 0 & 0 & kv & 0 \end{bmatrix} \qquad (49)$$

The eigenvalues of [A33 + B3 * K] can be obtained from

$$\det[sI - [A33 + B3 * K]] = 0.0 \qquad (50)$$

i.e.

$$s^4 + \left(\frac{c_g + \alpha}{J_g} + \frac{2 * \beta * k_d}{J_g} + \frac{2 * \alpha}{J_f} \right) * s^3$$

$$+ \left(\frac{2 * \alpha * (c_g + \alpha)}{J_g * J_f} + \frac{2 * \beta^2 * kd * kv}{J_f * J_g} + \frac{2 * \beta * kp}{J_g} \right) * s^2$$

$$+ \left(\frac{2 * \beta^2 * kp * kv}{J_f * J_g} + \frac{2 * \beta * ki}{J_g} \right) * s + \frac{2 * \beta^2 * ki * kv}{J_f * J_g} = 0$$

$$(51)$$

where

$$\alpha = (k_t * B_e)/R_a, \qquad (52)$$

$$\beta = (k_t * k_a)/R_a. \qquad (53)$$

For the dependence of the eigenvalues of [A33 + B3 * K] on ki, equation (51) can be rewritten as

$$1 + \frac{ki * (d * s + e)}{s^4 + a * s^3 + b * s^2 + c * s} = 0 \qquad (54)$$

Having introduced the augmented state, a small amount of ki is needed to bring one of the loci away from the origin. An extremely large ki could result in an unstable system as shown in Fig. 6. It is important to emphasize that ki is needed to eliminate any steady state error that may arise in the system. Assuming $u2 = 0.0$ and $\theta_{ref} = 0.0$, the steady state error due to a constant disturbance Lo can be shown to be

Fig. 6 Root locus for ki

Fig. 7 Root locus for kv

$$ek_{ss} = (-B_e * Lo)/(J_f * k_a * ki).\qquad(55)$$

For dependence of the eigenvalues of $[A33 + B3 * K]$ on kv, equation (51) can be rewritten as

$$1 + \frac{kv * (c * s^2 + e * s + f)}{s^2 + a * s^3 + b * s^2 + d * s} = 0 \qquad(56)$$

kv must be nonzero to remove one of the nondecaying modes which physically corresponds to the saturating flywheel. Figure 7 shows, however, that control kv should not be too large or else the response could become largely oscillatory. This suggests a narrow band control for the desaturation of the flywheel angular velocity.

Note that each root locus is drawn qualitatively based on the number of poles and zeroes of equation (54) and equation (56).

Using pole placement method, equation (51) can be used to find the gains kp, kd, ki, and kv. This may involve solving nonlinear equations because of cross terms between some of the gains.

A simpler and easier alternative is to solve for the more dominant gains kp and kd by first assuming ki and kv to be zero in equation (51). The desired locations of the poles are assigned and the following second-order equation:

$$s^2 \left(\frac{c_g + \alpha}{J_g} + \frac{2 * \beta * kd}{J_g} + \frac{2 * \alpha}{J_f} \right) * s$$

$$+ \left(\frac{2 * \alpha * (c_g + \alpha)}{J_g * J_f} + \frac{2 * \beta * kp}{J_g} \right) = 0 \qquad(57)$$

is then used to solve for kp and kd. Once kp and kd are computed, values for ki and kv can be assigned and equation (51) can be checked for all the four poles of the truncated dynamic system.

This simplication is reasonable and possible for two reasons.

(1) From the root locus diagrams, it is inferred that ki and kv should be small to avoid large oscillatory behavior.

(2) The primary control action would come from the effect of kp and kd, whereas kv is supposed to modulate the flywheel angular velocity and ki is supposed to remove steady-state disturbances.

4 Implementation of Discrete Time PID Control With Constant Desaturation of Flywheel Angular Velocity

The PID control with constant desaturation of the flywheel angular velocity designed in the continuous time domain is implemented by discretizing the controller with a backward rectangular approximation (BRA). A 1/3 second sampling time is found to be sufficient since the azimuth point system is a slow responding system. Several ad hoc schemes are also incorporated into the full implementation of the azimuth pointing system.

(1) A "bang-off" control with the RCUBE is used for coarse azimuth pointing. The objective is to prevent the flywheel from being accelerated to large angular velocity during large initial error. If the bang-on flag is "on" and if the computed error is larger than some preset band, then the RCUBE torque motor is driven with a constant voltage until the azimuth error falls within the preset band. Azimuth control is then switched over to the reaction wheel system.

(2) The desaturation control, eq. (41), is implemented with an offset grbase, i.e.,

$$u2 = \text{grbase} + kv * (\omega_f - \omega_{fref}), \qquad(58)$$

while a constant voltage gvolt is sent out to the gear motor. The magnitude of gvolt should be sufficient to maintain constant rotation of the bearing housing such that equation (14) or equation (15) is realized.

The polarity of each of the three quantities grbase, gvolt

and ω_{fref} are also assigned accordingly to insure the following conditions:

(a) that the direction of the reference flywheel velocity ω_{fref} corresponds to a preferred natural direction of rotation of the flywheel angular velocity;

(b) that grbase and gvolt have opposite polarity so that the RCUBE torque motor produces torque to counter the Coulomb friction torque brought about by driving the RCUBE gear motor with a constant gvolt (see equation (17)).

(3) As a slight deviation from normal integral control, sampling time is not multiplied into summed errors. This affects only the effective value of the gain ki. Maximum integrated command is limited in magnitude to 5 V.

(4) The effective command $u1$ is limited to 8.5 V absolute. This value is based on the actual hardware saturation level.

An Intel 80186 based computer with 8087 math processor is used to implement the controller. Azimuth angle information is derived from a strapdown inertial navigation unit called the Attitude Reference Unit (ARU).

5 Results of Azimuth Pointing for PID Control With Constant Desaturation of Flywheel Angular Velocity

Opportunities to fly the gondola are limited. Ground test provides verification of the effectiveness of the azimuth pointing. However, ground test conditions cannot duplicate flight conditions. Disturbance due to electrical cables hanging off the gondola, wind shear, type of hanging configurations affects the azimuth response. These disturbances are more significant during the transient part of the response.

The effectiveness of the azimuth controller is judged in terms of the steady state azimuth pointing performance and steady state maintenance of the flywheel angular velocity below saturation. In this regard, simulation, ground test and flight results show that these two criteria have been satisfied.

The following control parameters are used: $kp = 1174$, $kd = 894$, $ki = 10 * 3.0$, $kv = 0.03 * 9.55$; $|\text{mbang}| = 4.0$; $|\text{gvolt}| = 2.0$ V; $|\text{grbase}| = 1.6$ V; $\omega_{fref} = 70$ rpm during ground test and flight; $\omega_{fref} = 80$ rpm for simulation. The gains kp and kd are computed by using the dominant poles $(-1.25 \text{ s}^{-1} \pm 1.25 \text{ s}^{-1}\text{j})$ for equation (57). ki and kv are assigned accordingly.

In the following results, a trapezoidal scan trajectory is superimposed over the azimuth trajectory of a target. Slewing between scan points is conditioned by dividing large steps into many smaller steps. This is done to prevent saturating the azimuth controller which could result in unwanted transients.

Figure 8 shows a simulation result for azimuth tracking with scanning for the PID control. Steady state azimuth pointing rms is better than 0.01 deg. The flywheel velocity is maintained at around -56 rpm. Steady-state values for $u1$ and $u2$ are also of the same polarities indicating assistive production of torques. Coulomb friction settled at one direction except during the initial transients due to large slewing.

For the following two results, the values of control $u1$ and $u2$ and the flywheel angular velocity are recorded every 30 sampling loop due to limitations in the telemetry channels. Pointing performance in terms of the error average and error rms are quoted for each scan segment.

Figure 9 shows a ground test result for azimuth tracking with scanning for PID control. Steady state azimuth pointing rms is better than 0.02 deg for each scan segment. Flywheel velocity is maintained at around 60 rpm. Again the steady-state values of the control $u1$ and $u2$ have the same polarities. The magnitude of $u2$ is higher than that obtained with simulation indicating larger magnitude of friction disturbance.

Figure 10 shows a flight result for azimuth tracking with scanning for PID control. Steady state azimuth pointing rms is better than 0.02 deg for each scan segment. Flywheel velocity
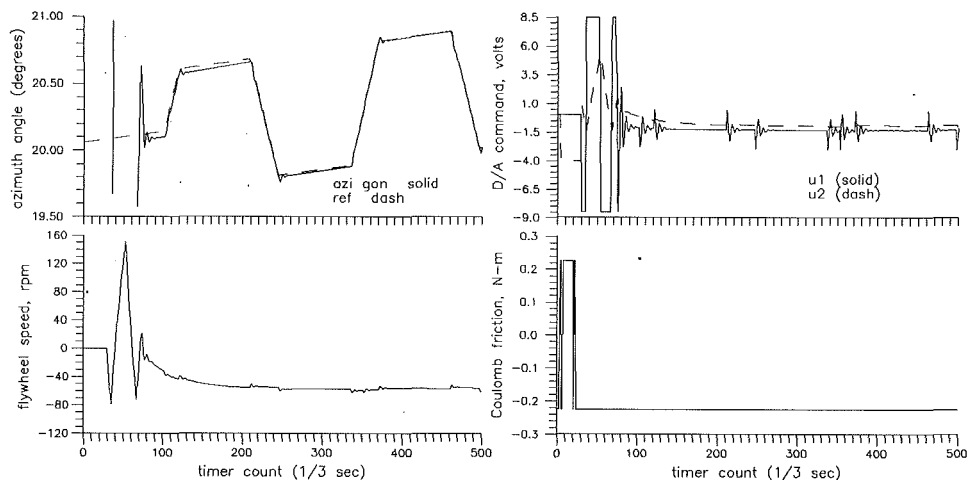
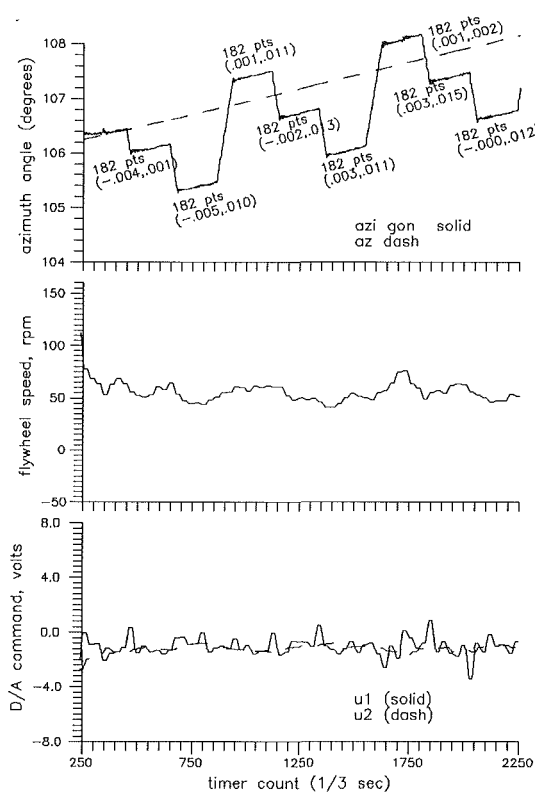**Fig. 8 Azimuth tracking with scanning, simulation result**

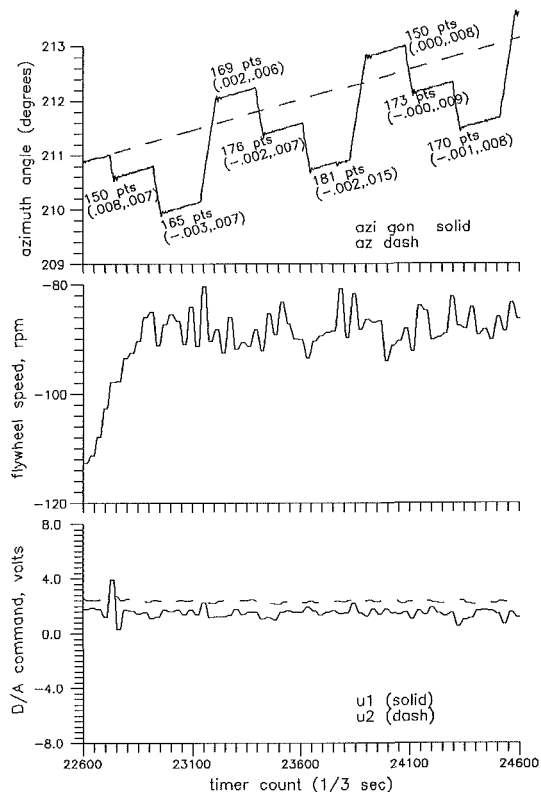**Fig. 9 Azimuth tracking with scanning, ground test result**

Fig. 10 Azimuth tracking with scanning, flight result

is maintained at around -85 rpm. $u1$ and $u2$ again producing assistive torque.

Results from the ground test and first flight show the same characteristic responses as that obtained during simulation.

continuous operation of the azimuth pointing system. Azimuth pointing rms is generally better than 0.02 deg and during flight 0.01 deg rms was achieved.

Model Reference Adaptive Control for the same azimuth pointing system has also been successfully developed and implemented. Results will be presented elsewhere.

Conclusions

Modeling of the azimuth pointing system of a balloon borne stabilized platform is presented. This model is successfully used for designing a PID control with constant desaturation of the flywheel angular velocity. Simulation results, ground test results, and actual flight results show that the controller can achieve the two control objectives of the azimuth pointing system, i.e., primary goal of achieving steady-state pointing rms of better than 0.1 deg and secondary goal of maintaining the flywheel angular velocity below saturation to provide for

Acknowledgment

References

Gibson, John, 1983, *Nonlinear Automatic Control*, McGraw-Hill Book Company, New York, pp. 454-464.

Greensite, Arthur, L., 1970, *Analysis and Design of Space Vehicle Flight Control Systems*, Spartan Books, New York, pp. 400-408, pp. 503-505.

Hazen, Nathan L., 1985, "Assuring Payload Security in Flight and Recovery: Design Approaches and Flight Experience," *Scientific Ballooning IV*, Vol. 5, No. 1, COSPAR, pp. 57-60.

Kailath, Thomas, 1980, *Linear System*, Prentice Hall, Inc., Englewood Cliffs, N.J.

Karnopp, Dean and Rosenberg, Ronald C., 1968, *Analysis and Simulation of Multiport Systems—The Bond Graph Approach to Physical System Dynamics*, The M.I.T. Press, M.I.T., Cambridge, Mass.

Nigro, N. J., Yang, J. K., and Elkouh, A. F., 1985, "Generalized Math Model for Simulation of High Altitude Balloon Systems," *Journal of Aircraft*, Vol. 22, No. 8, Aug., pp. 697-704.

Ogata, Katsuhiko, 1970, *Modern Control Engineering*, Prentice Hall, Inc., Englewood Cliffs, N.J.

Pelling, and Duttweiler, F., 1985, Private Communications, Physics Dept., UC, San Diego.